Geometry reconstruction of fluorescence detectors revisited

Daniel Kuempel, Karl-Heinz Kampert, Markus Risse

Department of Physics, Bergische Universität Wuppertal, Gaußstr. 20, D-42097 Wuppertal, Germany
Email: kuempel@physik.uni-wuppertal.de

***Abstract*— High-energy cosmic rays with energies exceeding 10^{17} eV are observed by measurements of the fluorescence light induced by air showers. In the fluorescence technique, the geometry of the shower is reconstructed from the correlation between arrival time and incident angle of the signals detected by the telescope. The calculation of the expected light arrival time used so far in shower reconstruction codes is based on several assumptions. Particularly, it is assumed that fluorescence photons are produced instantaneously during the passage of the shower front and that the fluorescence photons propagate on a straight line with vacuum speed of light towards the telescope. We investigate the validity of these assumptions, how to correct them, and the impact on reconstruction parameters when adopting realistic conditions. Depending on the relative orientation of the shower to the telescope, corrections can reach 100 ns in expected light arrival time, 0.1° in arrival direction and 5 g cm^{-2} in depth of shower maximum. The findings are relevant also for the case of "hybrid" observations where the shower is registered simultaneously by fluorescence and surface detectors.**

I. INTRODUCTION

The physics of the ultra-high energy (UHE) cosmic rays above 10^{19} eV is a challenging topic in the field of cosmic ray physics [1]. These cosmic rays are studied by detecting the atmospheric showers they initiate. Current and planned air shower experiments [2], [3], [4], [5], [6] use the technique of fluorescence light observation: shower particles deposit energy in the atmosphere through ionisational energy loss. Part of this energy (of order 10^{-4}) is emitted isotropically at near-UV wavelengths in de-excitation processes. These fluorescence photons can be detected by appropriate telescope systems operating in clear nights. Typically, pixel cameras with $25-100$ ns timing resolution are used, where an individual pixel covers a field of view of about $1-1.5°$ in diameter (see e.g. Ref. [2]). The signal (light flux per time) is registered as a function of the viewing direction of the pixels.

The first step to reconstruct the primary parameters of an observed air shower is given by the determination of the shower geometry. An accurate geometry reconstruction is, for instance, decisive for directional source searches; but it is also a prerequisite for reconstructing other important shower parameters such as the primary energy or the depth of shower maximum. We note that also the shower energies obtained from Auger ground array data are calibrated by the fluorescence telescopes [7].

The determination of the shower geometry is commonly performed in two steps in the fluorescence technique [9].

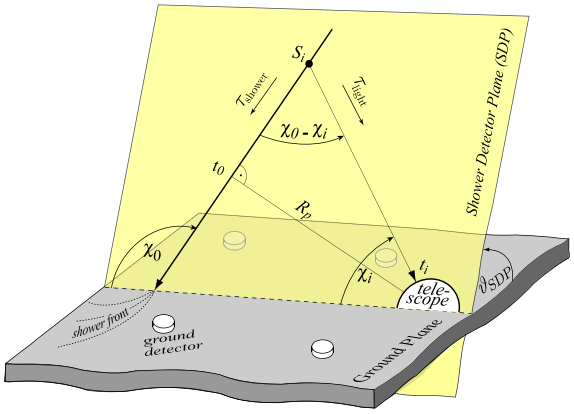

Fig. 1. Sketch of the shower geometry and quantities used in the derivations.

First, the "shower-detector-plane" (SDP) is determined as the plane spanned by the (signal-weighted) viewing directions of the triggered camera pixels (Fig. 1). Next, the geometry of the shower within this SDP is reconstructed based on the correlation between arrival time of the signals and viewing angle of the pixels projected into the SDP. The measured time-angle correlation is compared to the one expected for different shower geometries, and the best-fit geometry is determined. For the calculation of the expected time-angle correlation, the following function is in use (following e.g. Ref. [8], [9], [10]):

$$t_i = t_0 + \frac{R_p}{c_{\rm vac}} \tan\left(\frac{\chi_0 - \chi_i}{2}\right) \qquad (1)$$

where t_i is the arrival time of the photons at camera pixel i (usually, a signal-weighted average arrival time is taken from the time sequence observed in a pixel), t_0 is the time at which the shower axis vector passes the closest point to the telescope at a distance R_p, $c_{\rm vac}$ is the vacuum speed of light, χ_0 is the angle of incidence of the shower axis within the SDP, and χ_i is the viewing angle of pixel i within the SDP (see also Fig. 1). Comparing the expected $t_i - \chi_i$ correlation to the observed one ($i = 1...n$ for n triggered pixels), the best-fit parameters R_p, t_0 and χ_0 in Eq. (1) are found by a χ^2-minimization. Together with the SDP derived previously, the shower geometry is then fully determined and can also be expressed in terms of shower impact point, arrival direction, and ground impact time.

Eq. (1) is derived as follows. Assuming the fluorescence

light to be emitted by a point-like object moving at $c_{\rm vac}$ along the shower axis vector, the shower propagation time $\tau_{{\rm shower},i}$ from point S_i to the point at reference time t_0 on the shower axis (Fig. 1) can be expressed as

$$\tau_{{\rm shower},i} = \frac{R_p}{c_{\rm vac} \cdot \tan(\chi_0 - \chi_i)} \ . \qquad (2)$$

Next, assuming the fluorescence photons to propagate on straight lines with $c_{\rm vac}$, the light propagation time $\tau_{{\rm light},i}$ from S_i to the telescope is

$$\tau_{{\rm light},i} = \frac{R_p}{c_{\rm vac} \cdot \sin(\chi_0 - \chi_i)} \ . \qquad (3)$$

With Eqs. (2) and (3), and assuming an instantaneous emission of the fluorescence photons at S_i, the expected arrival time t_i (relative to the time t_0 of closest approach of the shower to the telescope) of fluorescence photons at a pixel viewing at an angle χ_i becomes

$$\begin{aligned} t_i &= t_0 - \tau_{{\rm shower},i} + \tau_{{\rm light},i} \\ &= t_0 + \frac{R_p}{c_{\rm vac}} \tan\left(\frac{\chi_0 - \chi_i}{2}\right) \end{aligned} \qquad (4)$$

which equals Eq. (1).

Thus, the derivation of Eq. (1) for calculating the expected time-angle correlation is based on the following assumptions:

- the spatial structure and the propagation of the shower disk can be approximated by a point-like object moving at $c_{\rm vac}$,
- the fluorescence light is produced instantaneously,
- the fluorescence light propagates with $c_{\rm vac}$,
- the fluorescence light propagates on a straight line.

In this article, we investigate the validity of these assumptions. The impact of the corrections on reconstruction parameters is studied. The results are relevant both for observations with fluorescence telescopes alone and for "hybrid" observations where the shower is registered by fluorescence and surface detectors.

This conference proceeding is based on a paper given in [11].

II. Analysis of individual effects

We discuss step-by-step the individual effects given by

- the spatial structure and speed of the shower disk (instead of a point-like object moving with $c_{\rm vac}$),
- the delayed (instead of instantaneous) fluorescence light emission,
- the reduced propagation speed of light (instead of $c_{\rm vac}$),
- the bending of light (instead of straight-line propagation).

A. Spatial structure and speed of shower disk

To check the assumption of the shower propagating as a point-like object with $c_{\rm vac}$ on a straight line, one may first regard the fastest particles during the cascading process. Assuming, as a rough estimate, an elasticity of 50% per interaction, the energy of the leading particle in a hadronic air shower is $E_{\rm lp} \simeq (E_0/A_0) \cdot 0.5^n$ after n interactions for a primary particle of energy E_0 and mass A_0. For $n = X_{\rm max}/\lambda \simeq 10$ (the depth of shower maximum in units of the hadronic interaction length), the energy of the leading particle is $\sim 10^{-3} E_0$ for primary protons and of order $\sim 10^{-5} E_0$ for primary iron. Hence, $E_{\rm lp} > 10^{13}$ eV for primary energies $E_0 > 10^{18}$ eV around shower maximum, which is the most relevant portion of the shower development for fluorescence light observations. In this case, the accumulated time delay of the leading particles with respect to an imaginary shower front moving with $c_{\rm vac}$ from the first interaction to $X_{\rm max}$ is $\ll$1 ns. This is negligible compared to current timing resolutions of giant shower detectors. Lateral deflections of these particles due to transverse momenta in interactions or deflection in the Earth's magnetic field are also sufficiently small (below $\sim$1 m).[1] For the case of UHE shower observations by fluorescence telescopes we conclude that the *fastest* shower particles can in reasonable approximation be assumed to move on a straight line along the shower axis with $c_{\rm vac}$.

The main contribution to the fluorescence signal in the shower, however, is due to lower-energy secondaries, particularly electrons and positrons between 0.1 MeV and several 100 MeV [12].[2] These have larger *lateral* displacements from the shower axis and larger *longitudinal* time delays with respect to the shower front.

Concerning the lateral width of the fluorescence shower beam, about 80% of the total fluorescence signal is produced within $\sim$75 m around the shower axis [12]. The impact of the finite shower width on the fluorescence reconstruction and how to correct it, was previously studied in detail [14]. It was shown in Ref. [14] that choosing too small a photon collection angle around the shower axis during reconstruction can lead to a signal loss and underestimation of the primary energy in nearby showers.

Here we study the longitudinal time delay of secondaries using the CORSIKA code [15]. In Fig. 2 the time delay of secondaries, weighted according to their contribution to the energy release into air and thus to the fluorescence signal, after the arrival time of the first particles is shown (10^{19} eV shower at maximum, for particles closer than 75 m from the axis; results are practically identical for primary proton and iron showers). One can note a sharp initial increase of the cumulative distribution (about 50% of energy is deposited within the first $3-4$ ns after the fastest particle), with a long tail towards larger delays. The average time delay is $\sim$8 ns, corresponding to a shower "thickness" of a few meters, which is in reasonable agreement with measurements of particle

[1] Time delay and lateral deflection of the leading particles may become non-negligible in case of considerably smaller E_0 or larger n (the latter being rather relevant for ground array observations of near-horizontal showers).

[2] Note that for the energy transfer from > 0.1 MeV electrons to fluorescence photons, the production of even lower-energy (e.g. $<$ 1 keV) electrons is important (for instance, the cross-section for exciting the main molecular bands (cf. Section II-B) has a sharp peak at about 20 eV electron energy). However, the additional delay from this intermediate step is $\ll$ 1 ns and, thus, negligible for this analysis [13].

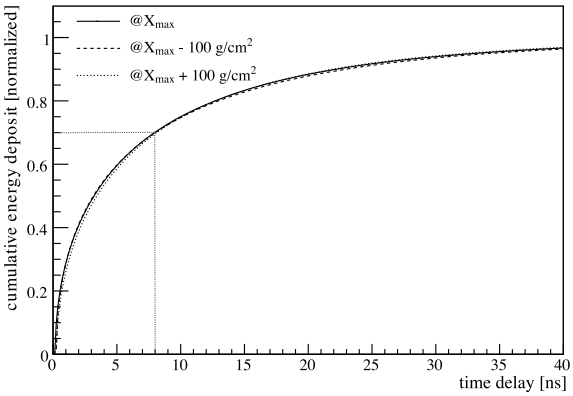

Fig. 2. Cumulative energy deposit (normalized to unity) as a function of time delay with respect to the fastest particle. The plot refers to a 10^{19} eV proton at shower maximum (and at 100 g cm^{-2} smaller/larger depths) and includes particles within 75 m of the shower axis. The average time delay is indicated by the dotted line. Simulations were performed with CORSIKA [15] / QGSJET 01 [17].

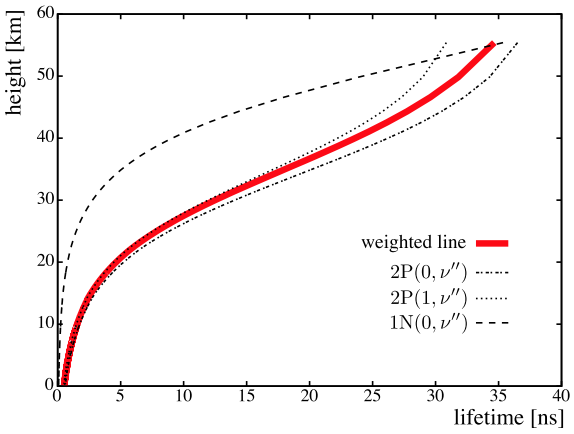

Fig. 3. Lifetime of the three main sets of bands as a function of height a.s.l. for dry air. The thick line shows the averaged lifetime, weighted according to different intensity fractions. The width of the line indicates the effect of a change in temperature by $\pm$40 K.

delays in air showers (see e.g. Ref. [16]). As can also be seen in Fig. 2, the distribution of time delays changes only marginally with the shower development stage.

The delay of secondaries with respect to the fastest shower particles results in a small constant time offset of the observed shower compared to the assumption of the shower moving with $c_{\rm vac}$. This might be less relevant for observations with fluorescence telescopes alone, since in this case, only the relative timing between the pixels is used to determine the spatial shower geometry. For hybrid observations, however, usually the arrival time of the first particle in the ground detector is taken, while in fluorescence telescopes, usually an average time from a fit to the signal viewed by a pixel is used. Then, comparing the timing signals from ground and fluorescence detectors, the small shift due to the finite shower thickness should be taken into account.[3] The precise value of the delay will depend on the specific procedure of signal extraction applied during reconstruction. As a rough estimate, the delay is of order $\tau_{\rm thick} \simeq 5{-}6$ ns.

To summarize, the leading particles in $>10^{18}$ eV showers can be considered to propagate along the shower axis with $c_{\rm vac}$, and one can set $\tau_{{\rm leading},i} \simeq \tau_{{\rm shower},i}$ with $\tau_{{\rm shower},i}$ given by Eq. (2). Compared to these particles, the secondaries relevant for the fluorescence light are slightly delayed due to the finite shower thickness by $\tau_{\rm thick}$, i.e. this term has to be added on the r.h.s. of Eq. (4).

B. Fluorescence light production

During propagation, the shower particles excite and ionize air molecules. Fluorescence light is then emitted by de-excitation and recombination.

Typical excitation times are of the order $\sim 10^{-6}$ ns [18] and negligible for current fluorescence telescopes. De-excitation times, in turn, can exceed 30 ns. Depending on the local atmospheric conditions and on the specific transition system, quenching processes (radiationless transitions by collisions with other molecules) can substantially reduce the mean de-excitation time of the radiative processes.

Fig. 3 shows the calculated lifetimes[4] as a function of height for the three main sets of bands [8] 2P$(0,\nu'')$, 2P$(1,\nu'')$ and 1N$(0,\nu'')$, assuming dry air (78.1% N_2, 20.9% O_2 and 1% Ar) and temperature profiles corresponding to the typical conditions at the Auger Observatory [20]. Also shown is the averaged lifetime, weighting the emission bands according to their relative (altitude dependent) intensities. The width of the weighted line indicates the effect of an arbitrary temperature variation of $\pm$40 K to show the minor dependence of the averaged lifetime on reasonable variations of the actual atmospheric conditions. At very high altitudes of 30$-$40 km, the averaged lifetime is 15$-$25 ns. With decreasing altitude, the quenching effect reduces the lifetime; thus, in general, the delay of fluorescence light emission with respect to the passing shower front is a differential effect that changes during the shower development (smaller delay deeper in the atmosphere).[5] At heights below $\sim$20 km where showers are typically observed by ground-based observatories, lifetimes of a few ns are reached.

The average lifetime $\tau_{\rm deexc}$ [in ns] (weighted line in Fig. 3) can in good approximation be parameterized as a function of height h a.s.l. [in m] of the emission point by

$$\tau_{\rm deexc}(h) = \frac{\tau_0}{\alpha \cdot e^{-h/H} + 1} \ , \qquad (5)$$

with $\tau_0 = 37.5$ ns, $H = 8005$ m and $\alpha = 95$. The term $\tau_{\rm deexc}(h)$ has to be added to the r.h.s. of Eq. (4).

C. Reduced speed of light

The propagation speed of light $v = c_{\rm vac}/n$ is reduced compared to the vacuum case by the local index of refraction

[3] For ground detectors located at larger distances from the shower axis, the curvature of the shower front needs to be accounted for in addition.

[4] A detailed description is given in [19]

[5] Anecdotally, this means the front of fluorescence light emission can move with an apparent velocity *larger* than $c_{\rm vac}$ through the atmosphere.

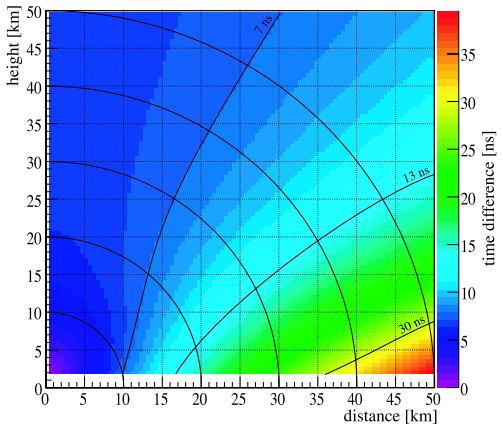

Fig. 4. Arrival time difference $(t_{\rm real} - t_{\rm vacuum})$ due to the effect of reduced speed of light. The telescope is placed at 1.4 km a.s.l. corresponding to the altitude of the Auger telescope station "Los Leones."

of air n. The change of n with wavelength is small (<3%) [21] within the fluorescence window of about 300−400 nm. A more detailed description is given in [11], [22].

In Fig. 4, the difference of light arrival times (between the cases of vacuum and reduced speed of light) is shown as a function of the location of emission point with respect to a telescope. The parametrization of $\rho(h)$ is taken from Ref. [20] for the example of the southern Auger Observatory. As expected, for fixed distance between emission point and telescope, time differences grow for propagation closer to ground due to the larger value of n. Differences of 20−25 ns or more can occur. For a single air shower, the effect changes along the longitudinal shower path, depending also on the relative orientation of shower axis and telescope. For instance, the time difference along the shower path typically varies less for showers pointing towards the telescope.

In Eq. (4), $\tau_{{\rm light},i}$ is replaced by $\tau_{{\rm refr},i}$. For convenience, one can express $\tau_{{\rm refr},i}$ using Eq. (3) by replacing $c_{\rm vac}$ with $c_{{\rm refr},i} = s/\tau_{\rm refr,i}$, defined as the effective speed of refracted light along the path of length s between emission point and telescope.

D. Bending of light

Due to refraction, the emitted light propagates on a bent trajectory. In turn, the direction of the incidence angle of the observed light does not point towards the real emission point, see Fig. 5 (right). More specifically, the zenith angle of downgoing light is continuously reduced during propagation.[6] The zenith angle difference $\Delta\vartheta = \vartheta_{\rm real} - \vartheta_{\rm app} \geq 0$ between the observed light direction $\vartheta_{\rm app}$ (towards the apparent emission point) and the straight-line direction $\vartheta_{\rm real}$ (towards the real emission point) has been calculated from ray tracing; it is shown in Fig. 5 (left) as a function of the position of the emission point in the atmosphere relative to the telescope. These shifts change over the longitudinal viewing direction towards an air shower. In case of hybrid observations where timing signals of fluorescence and ground detectors are combined, the impact time on ground estimated from the telescopes will be delayed compared to the actual one.

For a vertical shower, or, more generally, for showers with $\vartheta_{\rm SDP} = 90^\circ$ (cf. Fig. 1), χ_i in Eq. (4) is just reduced by $\Delta\vartheta$, as the refracted light direction still points towards the actual shower axis. In general, however, this effect slightly shifts the refracted light signals out of the actual SDP, and this shift usually changes along the shower path. Thus, the apparent SDP (which, in fact need not be a "plane" anymore) may slightly be tilted compared to the real one. To still permit the practical approach of fitting the best shower geometry within a plane only (instead of testing the full phase space), the projected shift $\Delta\vartheta \cdot \sin\vartheta_{\rm SDP}$ is taken as a correction. Thus, in Eq. (4), χ_i is replaced by $\chi_{{\rm refr},i} \simeq \chi_i - \Delta\vartheta_i \cdot \sin\vartheta_{\rm SDP}$ where $\chi_{{\rm refr},i}$ denotes the effective viewing direction of pixel i due to refraction. To account for the possible slight tilt of the apparent SDP, which is expected to be no larger than $\Delta\vartheta^{\rm max} \simeq$ (few times) 0.01°, the best-fit SDP might be found in an iterative procedure.

Finally, we note that the additional time delay due to the increased, bent path length compared to the straight-line connection (see sketch in Fig. 5) is $\ll$1 ns and can thus be neglected.

III. Impact on Shower Reconstruction

Taking the discussed effects into account, Eq. (1) is finally replaced by

$$t_i = t_0 - \frac{R_p}{c_{\rm vac}} \frac{1}{\tan(\chi_0 - \chi_{{\rm refr},i})} + \frac{R_p}{c_{{\rm refr},i}} \frac{1}{\sin(\chi_0 - \chi_{{\rm refr},i})} + \tau_{\rm thick} + \tau_{{\rm deexc},i} \quad (6)$$

The index i indicates that these quantities, for a given shower geometry, depend on the viewing direction of pixel i. One caveat, as discussed in Sec. II-D, is that the bending of light slightly changes the apparent SDP (within which the angles χ_0 and $\chi_{{\rm refr},i}$ are defined). It is worthwhile to note that all correction terms depend only on shower geometry but not on shower physics such as the primary particle type, which facilitates their application in shower reconstruction codes. $\tau_{\rm thick}$ can, to a good degree, be treated as a constant; $\tau_{{\rm deexc},i}$ depends on the altitude of the emission point; and $c_{{\rm refr},i}$ and $\chi_{{\rm refr},i}$ depend on the locations of emission point and telescope.

The time shifts introduced by the various effects along the viewing direction χ_i towards the shower are displayed in Fig. 6 for different shower geometries. The distance between impact point and telescope were fixed to 15 km (thin line) and 40 km (thick line), and for each distance three different

[6] We consider here only the case of a stable atmosphere with a standard decrease of $\rho(h)$ and $n(h)$ with height as given in Ref. [20]. We note, however, that the path of refracted light can become more complicated for specific atmospheric conditions such as atmospheric inversion, or in case of a strongly radiating ground leading to a local heating of air. The impact of the latter on the fluorescence technique might be reduced due to the fact that observations are only performed well (∼1−2 h) after / before sunset; also, the shower path very close to ground usually is below the field of view of the telescope (∼1° elevation of lower edge of field of view).

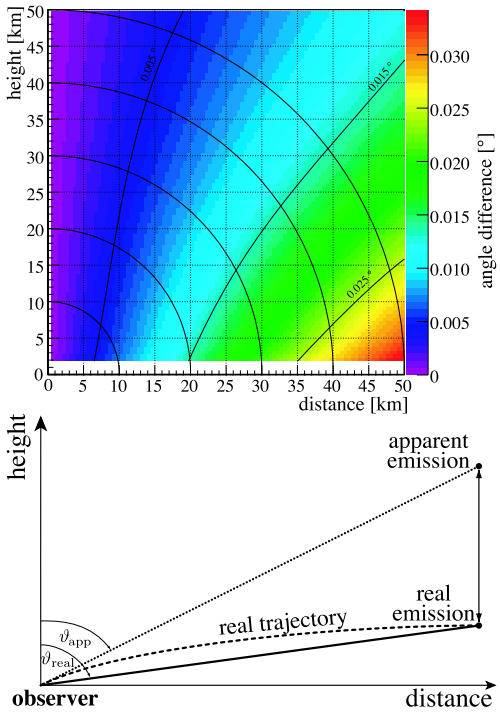

Fig. 5. Zenith angle difference $\Delta\vartheta = \vartheta_{\rm real} - \vartheta_{\rm app}$ between direct and curved path due to light refraction as a function of the location of the emission point relative to the telescope. The telescope is placed at 1.4 km a.s.l. corresponding to the altitude of the Auger telescope station "Los Leones."

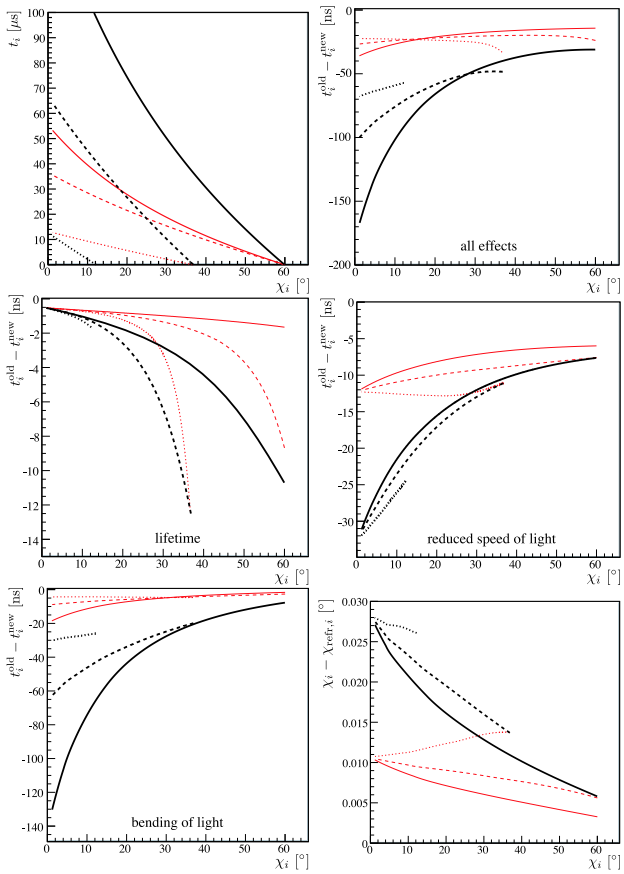

Fig. 6. Upper left plot: light arrival time t_i vs. light arrival angle (or pixel viewing direction) χ_i for different shower geometries (thick black (thin red) lines: shower impact point at 40 km (15 km) distance from the telescope; shower inclination χ_0 = 130° (solid), 90° (dashed), 50° (dotted); in all cases $\vartheta_{\rm SDP} = 90°$; shower track shown up to 50 km distance from the telescope). Upper right to lower left plot: differences in expected light arrival time for the given shower geometries between old and new reconstruction including all effects (upper right) and for individual effects as assigned. Lower right plot: differences of viewing angles towards apparent and actual emission point due to refraction.

shower inclinations of $\chi_0 = 50°, 90°, 130°$ are considered. Here, for simplicity $\vartheta_{\rm SDP} = 90°$ is taken such that $|90° - \chi_0|$ is identical to the shower zenith angle. In this case, the effect from light bending is minimized concerning the change of the SDP and maximized concerning $\chi_i - \chi_{{\rm refr},i}$.

In Fig. 6 (a), the overall shapes of t_i vs. χ_i are given, which differ for the different geometries. The shift of the arrival times, compared to the previous approach, is shown in Fig. 6 (b) when taking all effects into account. The contributions from the individual effects are provided in Figs. 6 (c)−(e). For the bending of light, in Fig. 6 (f), also the shift between apparent and effective viewing angle is given. One sees that the time delays are geometry dependent and can reach, and even exceed, 50−100 ns.

One also sees in Fig. 6 that the time delays change along the shower track in an individual event.

To investigate the effective impact of the corrections on the final reconstruction parameters, events were generated using CORSIKA [15] with the hadronic interaction model QGSJET 01 [17]. The shower sample consists of proton induced showers with energies of 10^{18}, 10^{19} and 10^{20} eV and zenith angles of 0, 45 and 60 deg (100 events per combination with random azimuth angles). The detector simulation and the event reconstruction was performed using the Auger software package described in [23], [24]. In terms of differences in arrival directions (the relevant quantity for directional source searches), differences are typically around 0.05°, but can exceed 0.1°. A systematic shift can be noted to slightly overestimate the shower zenith angles when neglecting the discussed effects, see Fig. 7. Shifts in energy are usually small ($\simeq$ 0.5−1% on average). Reconstructed values for the depth of shower maximum are typically changed by 2−3 g cm^{-2}, with a trend of the corrected $X_{\rm max}$ values being increased, and with larger corrections (5 g cm^{-2} and more) towards smaller values of the minimum viewing angle[7] (MVA).

IV. Conclusion

The assumptions used in the "classical" function of Eq. (1) for reconstructing the shower geometry from fluorescence light observations were investigated. The finite shower thickness leads to an energy deposition in air by secondaries which is delayed, compared to the shower front, by about 5−6 ns (with some dependence on the specific light collection algorithm employed). The emission of fluorescence light is further

[7]The MVA is defined as the smallest angle under which the reconstructed air shower is seen by the telescope.

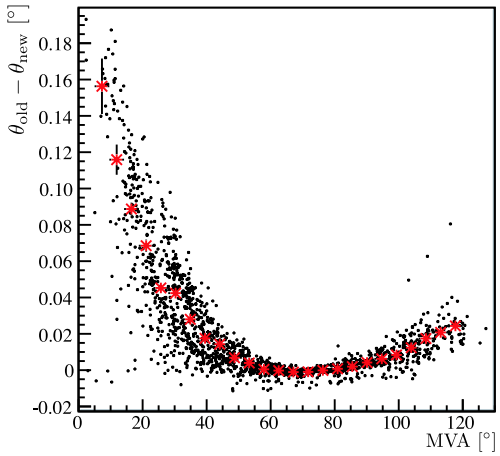

Fig. 7. Differences between old and new reconstruction in shower zenith angle as a function of the minimum viewing angle (dots indicate individual events, red stars the average value).

delayed due to the finite lifetime of the transitions which, due to quenching, is altitude dependent. Typical values are a few nanoseconds up to 20 km height, and >15 ns for heights above 30 km. The propagation speed of light is reduced by the index of refraction of air. The delay, compared to a propagation with vacuum speed of light, depends on the locations of emission point and telescope, and can exceed 20−25 ns. Finally, another effect of refraction is the bending of light, which also depends on the locations of emission point and telescope. Angular differences between the apparent and actual emission point of 0.02° can occur, which may correspond to time shifts of several 10 ns. This effect can also lead to a slight tilt of the SDP.

All these corrections can be considered as geometrical ones, i.e. they are independent of specific properties of the individual showers other than their geometry. The corrected function for geometry reconstruction is given in Eq. (6). Compared to the previous approach, which assumed maximum propagation speed of both light and particles as well as no other delays, the effects of delayed timing (including the effect of bending of light) accumulate. In total, differences of up to ∼100 ns in estimated light arrival time are possible. Air shower experiments with comparable, or better, time resolution should take these effects into account. This refers both to data reconstruction and to implementing these effects in the shower−detector simulation. In terms of overall shower reconstruction parameters, corrections are typically 0.03−0.05° in arrival direction (with a systematic trend of overestimating the zenith angle when neglecting the effect), ≃ 0.5−1% in energy and 2−3 g cm^{-2} in $X_{\rm max}$, but may in some cases exceed 0.1° and 5 g cm^{-2}. This is to be compared to typical reconstruction accuracies of ∼0.6° (directional resolution) [25] and ∼11 g cm^{-2} (systematic $X_{\rm max}$ uncertainty) [26] in case of Auger hybrid events.

The increase in computing time for event reconstruction is modest, particularly when applying the corresponding corrections only when approaching convergence in the minimization process (increase of ∼20% or less, depending on implementation). Some of the effects investigated in this work might be relevant also for shower detection techniques other than fluorescence telescope observations at ultra-high energy, e.g. Cherenkov light observations of air showers.

ACKNOWLEDGEMENTS

We would like to thank our Colleagues from the Pierre Auger Collaboration for many fruitful discussions, in particular Fernando Arqueros, Jose Bellido, Bruce Dawson, Philip Wahrlich and the members of the Auger group at the University of Wuppertal. Fig. 7 was produced using Auger software packages [23], [24]. This work was partially supported by the German Ministry for Research and Education (Grant 05 A08PX1).

REFERENCES

[1] M. Nagano, A.A. Watson, Rev. Mod. Phys. **72**, 689 (2000); "Ultimate energy particles in the Universe," eds. M. Boratav and G. Sigl, C.R. Physique **5**, Elsevier, Paris (2004); J. Cronin, Nucl. Phys. B, Proc. Suppl. **138** (2005), 465
[2] J. Abraham *et al.*, P. Auger Collaboration, Nucl. Instrum. Meth. **A 523**, 50 (2004)
[3] R.U. Abbasi *et al.*, Phys. Lett. B **619**, 271 (2005)
[4] M. Fukushima *et al.*, Prog. Theor. Phys. Suppl. **151**, 206 (2003)
[5] http://www.euso-mission.org
[6] http://owl.gsfc.nasa.gov
[7] M. Roth for the Pierre Auger Collaboration, Proc. 30$^{\rm th}$ Intern. Cosmic Ray Conf., Merida (2007); arXiv:0706.2096 [astro-ph]
[8] A. N. Bunner, "Cosmic Ray Detection by Atmospheric Fluorescence," Ph.D. thesis, Graduate School of Cornell University, (1967)
[9] R. M. Baltrusaitis *et al.*, Nucl. Instrum. Meth. A **240**, 410 (1985)
[10] P. Sokolsky, "Introduction to Ultrahigh Energy Cosmic Ray Physics," Addison-Wesley, Redwood City, USA (1989)
[11] D. Kuempel, K.-H. Kampert and M. Risse, Astropart. Phys. **30**, 167 (2008)
[12] M. Risse and D. Heck, Astropart. Phys. **20**, 661 (2004)
[13] F. Arqueros, *private communication* (2008)
[14] D. Góra *et al.*, Astropart. Phys. **24**, 484 (2006)
[15] D. Heck *et al.*, Reports **FZKA 6019 & 6097**, Forschungszentrum Karlsruhe (1998)
[16] G. Agnetta *et al.*, Astropart. Phys. **6**, 301 (1997)
[17] N.N. Kalmykov, S.S. Ostapchenko, A.I. Pavlov, Nucl. Phys. B (Proc. Suppl.) **52B**, 17 (1997)
[18] T. Waldenmaier, "Spectral resolved measurement of the nitrogen fluorescence yield in air induced by electrons," FZKA-7209, Forschungszentrum Karlsruhe, (2006)
[19] T. Waldenmaier *et al.*, Astropart. Phys. **29**, 205 (2008)
[20] B. Keilhauer *et al.* [Pierre Auger Collaboration], arXiv:astro-ph/0507275.
[21] K. Bernlöhr, Astropart. Phys. **12**, 255 (2000)
[22] R. C. Weast (ed.), "Handbook of Chemistry and Physics," 51st edition (Chemical Rubber Co., 1963) p. E-231
[23] S. Argiro *et al.*, Nucl. Instr. Meth. **A580**, 1485 (2007)
[24] L. Prado *et al.*, Nucl. Instr. Meth. **A545**, 632 (2005)
[25] C. Bonifazi for the Pierre Auger Collaboration, Proc. 29$^{\rm th}$ Intern. Cosmic Ray Conf., Pune, **7**, 17 (2005)
[26] M. Unger for the Pierre Auger Collaboration, Proc. 30$^{\rm th}$ Intern. Cosmic Ray Conf., Merida (2007); arXiv:0706.1495 [astro-ph]